

Enhancement of second-harmonic generation in BaTiO₃/SrTiO₃ superlattices

Tong Zhao, Zheng-Hao Chen,* Fan Chen, Wen-Sheng Shi, Hui-Bin Lu, and Guo-Zhen Yang
*Laboratory of Optical Physics, Institute of Physics, Center for Condensed Matter Physics, Chinese Academy of Sciences,
 P.O. Box 603, Beijing 100080, People's Republic of China*

(Received 16 February 1999)

Second-harmonic generation (SHG) of a 1.064- μm incident beam was investigated on BaTiO₃/SrTiO₃ superlattices prepared by laser molecular-beam epitaxy. The incidence angle and the polarization angle dependence of the SHG coefficients were measured. The SHG coefficients were greatly enhanced by the superlattice structure with the maximum value of $d_{33}=156.5$ pm/V being more than one order of magnitude larger than that of bulk BaTiO₃ crystal. The mechanism of SHG enhancement was discussed. [S0163-1829(99)02527-8]

To meet the need of the advanced electronic devices, many efforts have been made to enhance the dielectric and ferroelectric properties of ferroelectric materials with small dimensions. Being one of the most important ferroelectric perovskites, barium titanate (BaTiO₃) has attracted much attention. Recently, it has been found that the formation of the artificial superlattice of BaTiO₃/SrTiO₃ provided a powerful method for creating a new high-dielectric-constant material.^{1,2} By stacking ferroelectric BaTiO₃ (BTO) and paraelectric SrTiO₃ (STO) alternately, the dielectric constant ϵ_r were greatly enhanced and the high ϵ_r values were kept around a broad range of both total thickness and temperature because of the in-plane stress resulting from the lattice mismatch between BTO and STO. Besides its large ferroelectric and dielectric response, BTO is also a good optical nonlinear material. According to optical nonlinear principles, high refractive, i.e., high dielectric materials should have large nonlinear susceptibilities. Therefore, one can predict that the BTO/STO superlattice should exhibit large optical nonlinearity, which has the promise for applications in optical switches, filters, waveguides, and electro-optic devices. To our knowledge, however, little work has been done on nonlinear optical properties of the BTO/STO superlattice.

In the present work, we investigated the characteristics of the second-harmonic generation (SHG), the fundamental phenomenon in nonlinear optical effect, of a series of BTO/STO superlattices with various stacking periodicities n/m , where n and m are the numbers of BTO and STO unit-cell layer in one BTO(n)/STO(m) period, respectively, and found that the periodical structure enhances SHG greatly.

In this study, the BTO and STO layers were stacked alternately by a multitarget laser molecular-beam epitaxy (LMBE) technique. An XeCl excimer laser beam (308 nm, 20 ns, 2 Hz) was focused on the sintered BTO, or single crystal STO targets alternately with the pulsed energy intensity of about 1 J/cm². Monitored by the reflection high-energy electron diffraction (RHEED), the BTO or STO layers were deposited layer by layer on single-crystal SrTiO₃ (100) substrates. The deposition rate was about 0.01 nm/pulse. The thickness of each BTO or STO layer was varied in the range from 0.8 nm (2 unit cells) to 20 nm (50 unit cells) and the total thickness of the superlattices were

fixed at 80 nm (200 unit cells). The films were grown at 630 °C at an oxygen pressure of 1×10^{-4} Pa.

Crystallographic orientation and crystallinity of the deposited thin films were analyzed by either *in situ* RHEED patterns and the oscillations of their intensities or *ex situ* x-ray diffraction (XRD) patterns, atomic force microscopic (AFM), and high-resolution transmission electron microscopic (HRTEM) images. These results indicated that highly *c*-axis oriented BTO/STO superlattices were formed as designed with the root-mean-square roughness of 0.1 nm in surfaces and interfaces and in complete epitaxy with the substrates. Figure 1 shows the cross-sectional HRTEM micrograph of two periods of a BTO(20 unit cells)/STO(10 unit cells) superlattice, where there are 20 BTO unit cells and 10 STO unit cells in one period.

SHG data were collected using a typical setup with a signal and a reference channel.³ The TEM₀₀ output of a Q-switched Nd:YAG (yttrium aluminum garnet) laser with a wavelength of 1.064 μm was used as the fundamental beam. The laser pulse was incident on the superlattice mounted on a rotation stage, with a repetition rate of 5 Hz, a pulse duration of 20 ns, and a maximum energy of 50 mJ. The fundamental beam was split to pass through the signal and reference channels simultaneously. A piece of Z-cut quartz crystal (reference) was used in the reference channel for normalization against possible laser fluctuations. Another piece of

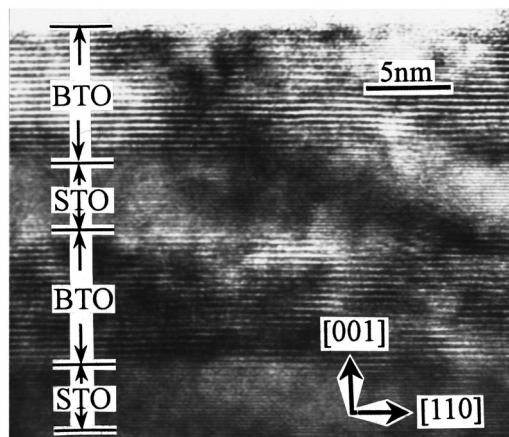


FIG. 1. Cross-sectional HRTEM micrograph of two periods of a BTO(20 unit cells)/STO(10 unit cells) superlattice.

Z-cut quartz crystal (calibration) was substituted for the superlattice specimen in the signal channel to allow the second-harmonic (SH) intensity from the superlattice to be scaled to the SHG coefficient $d_{11}=0.34$ pm/V of quartz. Selected by an analyzer placed before the photodetector, the p -polarized transmitted SH beam at 532 nm was measured as functions of both the incidence angle and the polarized angle of the fundamental beam. Each measured datum was obtained by a photomultiplier tube and by averaging the results of 100 laser shots using an instantaneous computer recording system. The thickness of the superlattice films (80 nm) was more than one order of magnitude less than the coherence length (3 μ m) of bulk BTO;⁴ hence the coherent factor in determining SHG coefficients can be ignored. Then the effective SHG coefficients for the superlattices can be approximately given by⁴

$$d_{\text{eff}} \approx \frac{l_q}{l_s} \left[\frac{n(2\omega)n^2(\omega)I_s T_q}{n_q(2\omega)n_q^2(\omega)I_q T_s} \right]^{1/2} d_{11}^q, \quad (1)$$

where $l_q=20$ μ m is the coherence length of quartz,³ l_s is the superlattice thickness, $n(2\omega)$ and $n(\omega)$ are the refractive indices of the superlattice at SH and fundamental frequencies, respectively, $n_q(2\omega)$ and $n_q(\omega)$ are the refractive indices of the quartz at each of the frequencies, I_s and I_q are the normalized SH intensities, T_s and T_q are the transmission factors for the superlattices and the calibration quartz, respectively, and $d_{11}^q=0.34$ pm/V is the optical nonlinear coefficient of quartz.³ According to our measurements, $T_s/T_q=0.8$. The refractive indices of BTO are similar to those of STO. So, we choose the refractive indices of BTO thin films as those of the BTO/STO superlattices, $n(2\omega)=2.2$, $n(\omega)=2.1$,⁵ $n_q(2\omega)n_q^2(\omega)=3.7$.⁶

By assuming the BTO/STO superlattices have approximately the same structure symmetry ($4mm$) of the bulk BTO crystal, the second-order nonlinear polarization can be expressed as

$$P^{\text{NL}} = \begin{pmatrix} 0 & 0 & 0 & 0 & d_{15} & 0 \\ 0 & 0 & 0 & d_{15} & 0 & 0 \\ d_{31} & d_{31} & d_{33} & 0 & 0 & 0 \end{pmatrix} \begin{pmatrix} E_x^2 \\ E_y^2 \\ E_z^2 \\ 2E_y E_z \\ 2E_z E_x \\ 2E_x E_y \end{pmatrix}. \quad (2)$$

Figures 2(a)–2(f) show the fundamental polarization dependence of effective SHG coefficients for a series of BTO/STO superlattices with stacking periodicity $n/m=2/2$, $4/4$, $10/10$, $20/20$, $30/30$, and $50/50$ unit cells, respectively. The incidence angle of the fundamental beam was chosen as 45° and the SH beam was p -polarized. The circle symbols represent experimental data. The solid lines are the best fits to the following function:

$$d_{\text{eff}} = |P^{\text{NL}}|/E^2 = d_1 \sin^2 \theta + d_2 \cos^2 \theta, \quad (3)$$

which can be derived from Eq. (2), where θ denotes the angle between the fundamental polarization and the incidence plane, d_1 and d_2 are linear functions of d_{15} , d_{31} , and d_{33} . The nearly perfect fits indicate that the assumption of

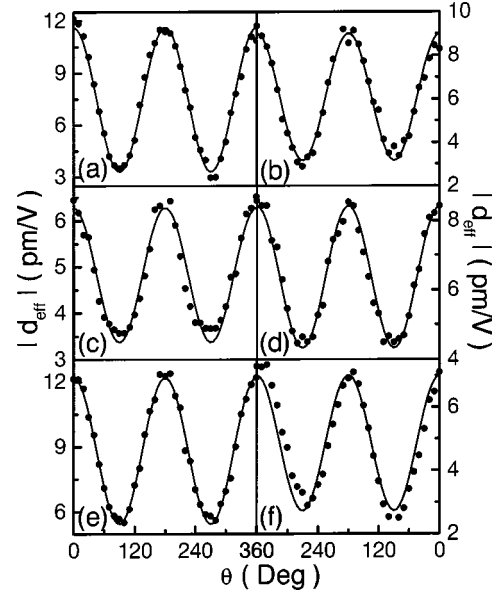


FIG. 2. Fundamental polarization dependence of the effective SHG coefficients of BTO/STO superlattices, with (a)–(f) being responsible for the stacking periodicity $n/m=2/2$, $4/4$, $10/10$, $20/20$, $30/30$, and $50/50$ unit cells, respectively. The incidence angle of the fundamental beam was chosen as 45° . The SH beam was p polarized. The circle symbols represent experimental data. The solid lines are the best fits to Eq. (3).

the BTO/STO superlattice with the same structure symmetry ($4mm$) of the bulk BTO is reasonable and these superlattices are isotropic in the plane of films. It should be noted that the maximum $|d_{\text{eff}}|$ values are much higher than the typical ones obtained from BTO films [2.13 pm/V (Ref. 4) and 0.8 pm/V (Ref. 5)].

To obtain the experimental values of d_{15} , d_{31} , and d_{33} for BTO/STO superlattices, the effective SHG coefficients as functions of the incidence angle α of the fundamental beam were measured. The fundamental and SH beams were selected as p -polarized. The results of $|d_{\text{eff}}|$ versus α are shown in Figs. 3(a)–3(f), which are responsible for the stacking periodicity $n/m=2/2$, $4/4$, $10/10$, $20/20$, $30/30$, and $50/50$ unit cells, respectively. The circle symbols represent experimental data. The zero values of $|d_{\text{eff}}|$ at the zero incidence angles are the characteristics of the c -axis oriented BTO films. The solid lines are the best fits to the following function:

$$d_{\text{eff}} = d_{15} \sin 2\alpha_\omega \cos \alpha_{2\omega} + (d_{31} \cos^2 \alpha_\omega + d_{33} \sin^2 \alpha_\omega) \sin \alpha_{2\omega}, \quad (4)$$

which can be derived from Eq. (2). Here α_ω and $\alpha_{2\omega}$ are the internal angles of fundamental and SH beams, respectively, which are given by $n(\omega)\sin \alpha_\omega = \sin \alpha = n(2\omega)\sin \alpha_{2\omega}$ with $n(\omega)$ and $n(2\omega)$ being the refractive indices at the fundamental and SH frequencies, respectively. The fitting results of d_{15} , d_{31} , and d_{33} for a series of BTO/STO superlattices with various stacking periodicities are listed in Table I, where those values of the bulk BTO crystal and the BTO thin film obtained by other authors⁶ are included for comparison.

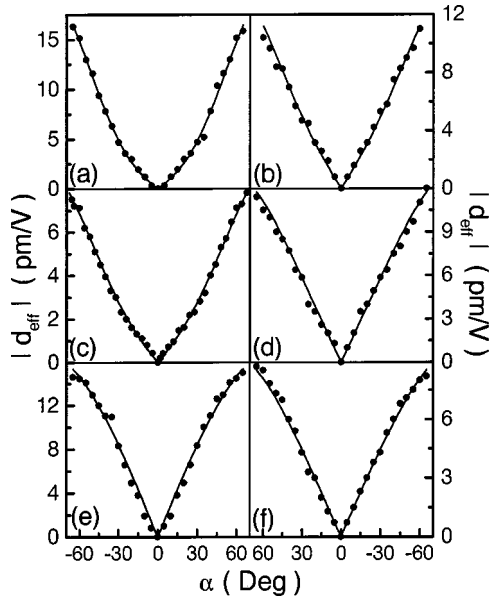


FIG. 3. Fundamental incidence angle dependence of the effective SHG coefficients of BTO/STO superlattices, with (a)–(f) being responsible for the stacking periodicity $n/m=2/2, 4/4, 10/10, 20/20, 30/30,$ and $50/50$ unit cells, respectively. The fundamental and SH beam were p polarized. The circle symbols represent experimental data. The solid lines are the best fits to Eq. (4).

From the fitting results, we can see that, for BTO/STO superlattices with various stacking periodicities, d_{15} is lower than that of the bulk BTO crystal, d_{31} is almost the same as, and d_{33} is much larger than those of the bulk BTO crystal, while they are all much larger than the typical BTO thin-film values reported by other authors. It should be noted that d_{33} has been dramatically enhanced with the maximum value being more than one order of magnitude larger than that of the bulk BTO crystal and it increases with decreasing the stacking periodicity.

The results above clearly show that the formation of the BTO/STO superlattice greatly enhances SHG from BTO. The enhancement can be attributed to several factors.

Bulk BTO has a perovskite-type tetragonal structure with point-group symmetry $4mm$, which is responsible for its ferroelectric and second-order optical nonlinear properties. Bulk STO has a cubic structure with point-group symmetry $m3m$, which is responsible for its paraelectric and non-

TABLE I. SHG coefficients of various BTO/STO superlattices with various stacking periodicities.

Stacking periodicity n/m (unit cells)	d_{15} (pm/V)	d_{31} (pm/V)	d_{33} (pm/V)
2/2	2.3	8.5	156.5
4/4	3.1	12.0	76.8
10/10	1.1	7.3	55.6
20/20	4.5	14.9	46.6
30/30	9.3	17.3	38.6
50/50	4.2	10.8	27.0
BTO bulk crystal	17.0	15.7	6.8
BTO thin film	2.2	2.1	0.90

second-order optical nonlinear properties. The lattice constants of bulk BTO and STO are $a=b=0.3990$ nm, $c=0.4036$ nm, and $a=b=c=0.3905$ nm, respectively.¹ Therefore, inside the BTO/STO superlattice, compression (expansion) and expansion (compression) stress are expected to be introduced along the interface and perpendicular to the interface in BTO (STO) layers resulting from the lattice mismatch between BTO and STO. So, in the c -axis oriented superlattices, the c axis was enlarged while the a axis was shortened for BTO layers. The lattice constant c of the BTO layers increases, while the lattice constant a decreases with decreasing stacking periodicity and reach their extremum values at the stacking periodicity $n/m=2/2$ unit cells. That is, a large stress ($\sim 10^9$ Pa)¹ was introduced into the BTO layers. Resulting from this stress, the tetragonal phase of BTO was stabilized, the spontaneous polarization \mathbf{P}_s was increased, and the dielectric constant ϵ_r of BTO was enhanced with the same tendency as that of the lattice constant c and having the maximum value of 900 at the 2 unit cell/2 unit cell structure. The coefficient of SHG, d_{ijk} , can be expressed as $d_{ijk} \propto \chi_{ii}^{2\omega} \chi_{jj}^{\omega} \chi_{kk}^{\omega}$, where χ^{ω} and $\chi^{2\omega}$ are the linear optical susceptibilities at frequencies of ω and 2ω , respectively,⁷ and $\chi = (\epsilon_r - 1)/4\pi$. So one can deduce that d_{ijk} was enhanced with the same tendency as that of ϵ_r .

In addition to the spontaneous polarization \mathbf{P}_s , the large stress in the BTO/STO superlattice can also produce an additional polarization \mathbf{P} through the piezoelectric effect, which would produce SHG in the same way as does the spontaneous polarization \mathbf{P}_s .⁵ \mathbf{P} normal to the film surface would produce c -axis-oriented-like SHG. Using the stress given above and piezoelectric coefficients from Ref. 8, the value of \mathbf{P} normal to the film surface produced by the stress in BTO layers through piezoelectric effect can be estimated to about 0.2 C/m², which is comparable with that of \mathbf{P}_s in bulk BTO crystal,⁹ 0.25 C/m². Hence, SHG may be enhanced by the stress in BTO layers through the piezoelectric effect.

Considering the enhancement of spontaneous and stress-induced polarizations and the enlargement of lattice constant of BTO layers being in the direction of c axis, the anisotropic enhancement of d_{15} , d_{31} , and d_{33} can be understood. The SHG coefficient d_{ijk} is proportional to the ensemble average of $r_i r_j r_k$, with r_i being the dipole moment operator in the i direction. Therefore, one should expect for the largest enhancement in $d_{33}(d_{ccc})$, and the small ones in $d_{15}(d_{aca})$ and $d_{31}(d_{caa})$.

Besides the contribution of polarization, the enhancement of SHG can also be attributed to the interfaces in BTO/STO superlattices. It has been found that the interfaces can produce SHG even in centrosymmetry semiconductor superlattices.¹⁰ One can expect that the interfaces in BTO/STO superlattices may be responsible for a part of SHG.

Besides the explanation mentioned above, there may be two other reasons responsible for the enhancement of SHG. The first is the contribution of STO layers in BTO/STO superlattices. The bulk STO crystal is cubic, which cannot generate SH. In the BTO/STO superlattice, however, STO layers also strained due to the lattice mismatch. Without centrosymmetry, the strained STO layers may also generate SH. The second is the good crystallinity of the samples. As confirmed by XRD, AFM, and HRTEM, the BTO/STO superlattices

used in this study were in complete epitaxy with the substrates with the root-mean-square roughness of only 0.1 nm in surfaces and interfaces, which may allow the superlattice thin films perform as single crystal.

From the discussion above, one can see that there are two conflicting factors affecting SHG in BTO/STO superlattices. The smaller the stacking periodicity was, the larger the stress and the polarization were introduced into the BTO layers, and the more the interfaces were involved, which can enhance SHG. On the other hand, the smaller the stacking periodicity was, the more the deviation of the BTO layers were from the bulk structure, which can reduce SHG. The resultant SHG is the balance of these two factors, which is responsible for the varying tendency in d_{33} and the anisotropic enhancement among d_{15} , d_{31} , and d_{33} .

In conclusion, BTO/STO superlattices with various stack-

ing periodicities were grown by LMBE. The fundamental polarization dependence and the incidence angle dependence of SHG from these superlattices have been measured systematically. The data of experiments and theoretical fitting show that the SHG coefficients, especially d_{33} , were greatly enhanced by the formation of the BTO/STO superlattice with the maximum value being more than one order of magnitude larger than that of the bulk BTO crystal. The enhancement of SHG has been attributed to the enhancement of polarization, the introduced interfaces, the contribution of strained STO layers, and the good crystallinity. From the results above, it indicates that the BTO/STO superlattice may be very promising for nonlinear optical applications.

This work was supported by the Ministry for Science and Technology of China.

*Electronic address: zhchen@aphy.iphy.ac.cn

¹Hitoshi Tabata and Tomoji Kawai, *Appl. Phys. Lett.* **70**, 321 (1997).

²Hitoshi Tabata, Hidekazu Tanaka, and Tomoji Kawai, *Appl. Phys. Lett.* **65**, 1970 (1994).

³H. A. Lu, L. A. Wills, B. W. Wessels, W. P. Lin, T. G. Zhang, G. K. Wong, D. A. Neumayer, and T. T. Marks, *Appl. Phys. Lett.* **62**, 1314 (1993).

⁴Bipin Bihari, Jayant Kumar, Gregory T. Stauff, Peter C. Van Buskirk, and Cheol Seong Hwang, *J. Appl. Phys.* **76**, 1169 (1994).

⁵L. D. Rotter, D. L. Kaiser, and M. D. Vaudin, *Appl. Phys. Lett.* **68**, 310 (1996).

⁶Tatsuo Okada, Yoshiaki Nakata, Hiroshi Kaibara, and Mitsuo

Maeda, *Jpn. J. Appl. Phys., Part 2* **34**, L1536 (1995).

⁷Y. R. Shen, *The Principles of Nonlinear Optics* (Wiley, New York, 1984), p. 37.

⁸T. Ikeda, E. Nakamura, S. Nomura, E. Sawaguchi, Y. Shiozaki, and K. Toyoda, in *Numerical Data and Functional Relationships in Science and Technology*, edited by K.-H. Hellwege and A. M. Hellwege, Landolt-Börnstein, New Series, Group III, Vol. 3 (Springer-Verlag, Berlin, 1981), p. 55.

⁹M. DiDomenico, Jr. and S. H. Wemple, *J. Appl. Phys.* **40**, 720 (1969).

¹⁰Xudong Xiao, Chun Zhang, A. B. Fedotov, Zhenghao Chen, and M. M. T. Loy, *J. Vac. Sci. Technol. B* **15**, 1112 (1997).